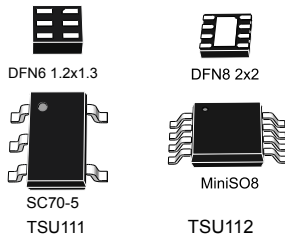


Nanopower (900 nA), high accuracy (150 μ V) 5 V CMOS operational amplifier



Features

- Sub-micro ampere current consumption: $I_{CC} = 900$ nA typ. at 25 °C
- Low offset voltage: 150 μ V max. at 25 °C, 235 μ V max. over full temperature range (-40 to 85 °C)
- Low noise over 0.1 to 10 Hz bandwidth: 3.6 μ Vpp
- Low supply voltage: 1.5 V to 5.5 V
- Rail-to-rail input and output
- Gain bandwidth product: 11.5 kHz typ.
- Low input bias current: 10 pA max. at 25 °C
- High tolerance to ESD: 4 kV HBM
- More than 25 years of typical equivalent lifetime supplied by a 220 mA.h CR2032 coin type Lithium battery
- High accuracy without calibration
- Tolerance to power supply transient drops

Applications

- Gas sensors: CO, O₂, and H₂S
- Alarms: PIR sensors
- Signal conditioning for energy harvesting and wearable products
- Ultra long-life battery-powered applications
- Battery current sensing
- Active RFID tags

Description

The **TSU111**, **TSU112** operational amplifiers (op-amp) offer an ultra low-power consumption per channel of 900 nA typical and 1.2 μ A maximum when supplied by 3.3 V. Combined with a supply voltage range of 1.5 V to 5.5 V, these features allow the TSU11x to be efficiently supplied by a coin type Lithium battery or a regulated voltage in low-power applications.

The high accuracy of 150 μ V max. and 11.5 kHz gain bandwidth make the TSU11x ideal for sensor signal conditioning, battery supplied, and portable applications.

Product status link

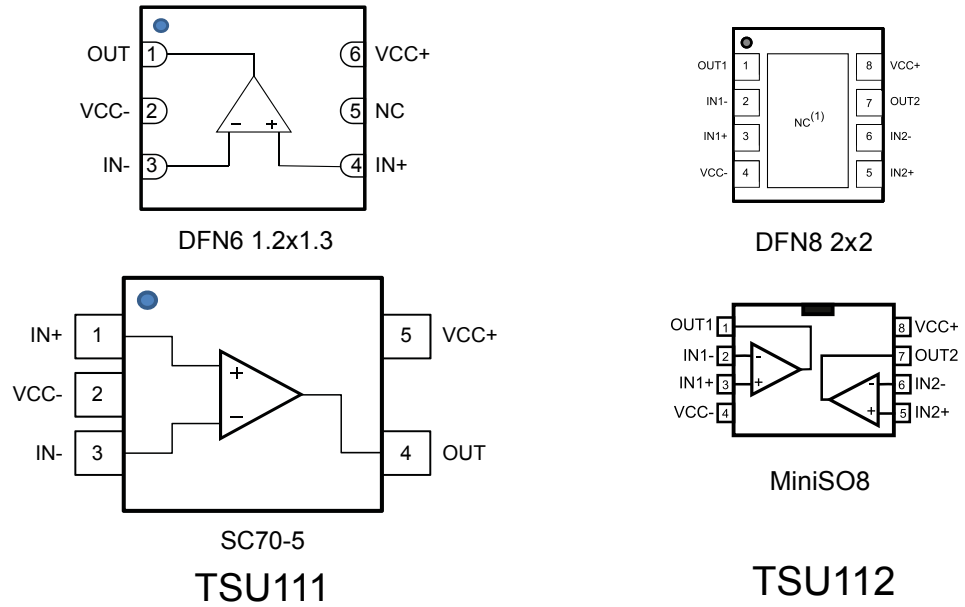
[TSU111, TSU112](#)

Related products

See TSU101 , TSU102 , and TSU104	for further power savings
See TSZ121 , TSZ122 , and TSZ124	for increased accuracy

1 Package pin connections

Figure 2. Pin connections for each package (top view)



1. The exposed pad of the DFN8 2x2 can be connected to V_{CC-} or left floating.

2 Absolute maximum ratings and operating conditions

Table 1. Absolute maximum ratings (AMR)

Symbol	Parameter	Value	Unit	
V_{CC}	Supply voltage ⁽¹⁾	6	V	
V_{id}	Differential input voltage ⁽²⁾	$\pm V_{CC}$		
V_{in}	Input voltage ⁽³⁾	$(V_{CC-}) - 0.2$ to $(V_{CC+}) + 0.2$		
I_{in}	Input current ⁽⁴⁾	10	mA	
T_{stg}	Storage temperature	-65 to 150	°C	
T_j	Maximum junction temperature	150		
R_{thja}	Thermal resistance junction-to-ambient ^{(5) (6)}	DFN6 1.2x1.3	232	°C/W
		SC70-5	205	
		DFN8 2x2	57	
		MiniSO8	190	
ESD	HBM: human body model ⁽⁷⁾	4000	V	
	CDM: charged device model ⁽⁸⁾	1500		
	Latch-up immunity ⁽⁹⁾	200	mA	

1. All voltage values, except the differential voltage are with respect to the network ground terminal.
2. The differential voltage is the non-inverting input terminal with respect to the inverting input terminal.
3. $(V_{CC+}) - V_{in}$ must not exceed 6 V, $V_{in} - (V_{CC-})$ must not exceed 6 V.
4. The input current must be limited by a resistor in-series with the inputs.
5. R_{th} are typical values.
6. Short-circuits can cause excessive heating and destructive dissipation.
7. Related to ESDA/JEDEC JS-001 Apr. 2010.
8. Related to JEDEC JESD22-C101-E Dec. 2009.
9. Related to JEDEC JESD78C Sep. 2010.

Table 2. Operating conditions

Symbol	Parameter	Value	Unit
V_{CC}	Supply voltage	1.5 to 5.5	V
V_{icm}	Common-mode input voltage range	$(V_{CC-}) - 0.1$ to $(V_{CC+}) + 0.1$	
T_{oper}	Operating free-air temperature range	-40 to 85	°C

3 Electrical characteristics

Table 3. Electrical characteristics at $(V_{CC+}) = 1.8\text{ V}$ with $(V_{CC-}) = 0\text{ V}$, $V_{icm} = V_{CC}/2$, $T_{amb} = 25\text{ °C}$, and $R_L = 1\text{ M}\Omega$ connected to $V_{CC}/2$ (unless otherwise specified)

Symbol	Parameter	Conditions	Min.	Typ.	Max.	Unit
DC performance						
V_{io}	Input offset voltage	$T = 25\text{ °C}$			150	μV
		$-40\text{ °C} < T < 85\text{ °C}$			235	
$\Delta V_{io}/\Delta T$	Input offset voltage drift	$-40\text{ °C} < T < 85\text{ °C}$			1.4	$\mu\text{V}/\text{°C}$
ΔV_{io}	Long-term input offset voltage drift	$T = 25\text{ °C}$ ⁽¹⁾		TBD		$\mu\text{V}/\sqrt{\text{month}}$
I_{io}	Input offset current ⁽²⁾	$T = 25\text{ °C}$		1	10	pA
		$-40\text{ °C} < T < 85\text{ °C}$			50	
I_{ib}	Input bias current ⁽²⁾	$T = 25\text{ °C}$		1	10	pA
		$-40\text{ °C} < T < 85\text{ °C}$			50	
CMR	Common mode rejection ratio, $20 \log(\Delta V_{icm}/\Delta V_{io})$, $V_{icm} = 0$ to 1.8 V	$T = 25\text{ °C}$	76	107		dB
		$-40\text{ °C} < T < 85\text{ °C}$	71			
A_{vd}	Large signal voltage gain, $V_{out} = 0.2\text{ V}$ to $(V_{CC+}) - 0.2\text{ V}$	$R_L = 100\text{ k}\Omega$, $T = 25\text{ °C}$	95	120		dB
		$R_L = 100\text{ k}\Omega$, $-40\text{ °C} < T < 85\text{ °C}$	90			
V_{OH}	High-level output voltage, (drop from V_{CC+})	$R_L = 10\text{ k}\Omega$, $T = 25\text{ °C}$		10	25	mV
		$R_L = 10\text{ k}\Omega$, $-40\text{ °C} < T < 85\text{ °C}$			40	
V_{OL}	Low-level output voltage	$R_L = 10\text{ k}\Omega$, $T = 25\text{ °C}$		8	25	mV
		$R_L = 10\text{ k}\Omega$, $-40\text{ °C} < T < 85\text{ °C}$			40	
I_{out}	Output sink current, $V_{out} = V_{CC}$, $V_{ID} = -200\text{ mV}$	$T = 25\text{ °C}$	2.8	5		mA
		$-40\text{ °C} < T < 85\text{ °C}$	1.5			
	Output source current, $V_{out} = 0\text{ V}$, $V_{ID} = 200\text{ mV}$	$T = 25\text{ °C}$	2	4		
		$-40\text{ °C} < T < 85\text{ °C}$	1.5			
I_{CC}	Supply current (per channel), no load, $V_{out} = V_{CC}/2$	$T = 25\text{ °C}$		900	1200	nA
		$-40\text{ °C} < T < 85\text{ °C}$			1480	
AC performance						
GBP	Gain bandwidth product	$R_L = 1\text{ M}\Omega$, $C_L = 60\text{ pF}$		10		kHz
F_u	Unity gain frequency			8		
Φ_m	Phase margin			60		degrees
G_m	Gain margin			10		dB

Symbol	Parameter	Conditions	Min.	Typ.	Max.	Unit
SR	Slew rate (10 % to 90 %)	$R_L = 1 \text{ M}\Omega$, $C_L = 60 \text{ pF}$, $V_{out} = 0.3 \text{ V to } (V_{CC+}) - 0.3 \text{ V}$		2.5		V/ms
e_n	Equivalent input noise voltage	$f = 100 \text{ Hz}$		220		nV/ $\sqrt{\text{Hz}}$
f_{e_n}	Low-frequency, peak-to-peak input noise	Bandwidth: $f = 0.1 \text{ to } 10 \text{ Hz}$		3.8		μV_{pp}
t_{rec}	Overload recovery time	100 mV from rail in comparator, $R_L = 100 \text{ k}\Omega$, $V_{ID} = \pm 1 \text{ V}$, $-40 \text{ }^\circ\text{C} < T < 85 \text{ }^\circ\text{C}$		325		μs

1. Typical value is based on the V_{io} drift observed after 1000h at 85 °C extrapolated to 25 °C using the Arrhenius law and assuming an activation energy of 0.7 eV. The operational amplifier is aged in follower mode configuration
2. Guaranteed by design

Table 4. Electrical characteristics at (V_{CC+}) = 3.3 V with (V_{CC-}) = 0 V, $V_{icm} = V_{CC}/2$, $T_{amb} = 25 \text{ }^\circ\text{C}$, and $R_L = 1 \text{ M}\Omega$ connected to $V_{CC}/2$ (unless otherwise specified)

Symbol	Parameter	Conditions	Min.	Typ.	Max.	Unit
DC performance						
V_{io}	Input offset voltage	$T = 25 \text{ }^\circ\text{C}$			150	μV
		$-40 \text{ }^\circ\text{C} < T < 85 \text{ }^\circ\text{C}$			235	
$\Delta V_{io}/\Delta T$	Input offset voltage drift	$-40 \text{ }^\circ\text{C} < T < 85 \text{ }^\circ\text{C}$			1.4	$\mu\text{V}/^\circ\text{C}$
ΔV_{io}	Long-term input offset voltage drift	$T = 25 \text{ }^\circ\text{C}$ ⁽¹⁾		TBD		$\mu\text{V}/\sqrt{\text{month}}$
I_{io}	Input offset current ⁽²⁾	$T = 25 \text{ }^\circ\text{C}$		1	10	pA
		$-40 \text{ }^\circ\text{C} < T < 85 \text{ }^\circ\text{C}$			50	
I_{ib}	Input bias current ⁽²⁾	$T = 25 \text{ }^\circ\text{C}$		1	10	pA
		$-40 \text{ }^\circ\text{C} < T < 85 \text{ }^\circ\text{C}$			50	
CMR	Common mode rejection ratio, $20 \log (\Delta V_{icm}/\Delta V_{io})$, $V_{icm} = 0 \text{ to } 3.3 \text{ V}$	$T = 25 \text{ }^\circ\text{C}$	81	110		dB
		$-40 \text{ }^\circ\text{C} < T < 85 \text{ }^\circ\text{C}$	76			
A_{vd}	Large signal voltage gain, $V_{out} = 0.2 \text{ V to } (V_{CC+}) - 0.2 \text{ V}$	$R_L = 100 \text{ k}\Omega$, $T = 25 \text{ }^\circ\text{C}$	105	130		dB
		$R_L = 100 \text{ k}\Omega$, $-40 \text{ }^\circ\text{C} < T < 85 \text{ }^\circ\text{C}$	105			
V_{OH}	High-level output voltage, (drop from V_{CC+})	$R_L = 10 \text{ k}\Omega$, $T = 25 \text{ }^\circ\text{C}$		10	25	mV
		$R_L = 10 \text{ k}\Omega$, $-40 \text{ }^\circ\text{C} < T < 85 \text{ }^\circ\text{C}$			40	
V_{OL}	Low-level output voltage	$R_L = 10 \text{ k}\Omega$, $T = 25 \text{ }^\circ\text{C}$		7	25	mV
		$R_L = 10 \text{ k}\Omega$, $-40 \text{ }^\circ\text{C} < T < 85 \text{ }^\circ\text{C}$			40	
I_{out}	Output sink current, $V_{out} = V_{CC}$, $V_{ID} = -200 \text{ mV}$	$T = 25 \text{ }^\circ\text{C}$	12	22		mA
		$-40 \text{ }^\circ\text{C} < T < 85 \text{ }^\circ\text{C}$	6			
	Output source current, $V_{out} = 0 \text{ V}$, $V_{ID} = 200 \text{ mV}$	$T = 25 \text{ }^\circ\text{C}$	9	18		
		$-40 \text{ }^\circ\text{C} < T < 85 \text{ }^\circ\text{C}$	5			
I_{CC}	Supply current (per channel), no load, $V_{out} = V_{CC}/2$	$T = 25 \text{ }^\circ\text{C}$		900	1200	nA
		$-40 \text{ }^\circ\text{C} < T < 85 \text{ }^\circ\text{C}$			1480	
AC performance						

Symbol	Parameter	Conditions	Min.	Typ.	Max.	Unit
GBP	Gain bandwidth product	$R_L = 1\text{ M}\Omega, C_L = 60\text{ pF}$		11		kHz
F_u	Unity gain frequency			10		
Φ_m	Phase margin			60		degrees
G_m	Gain margin			7		dB
SR	Slew rate (10 % to 90 %)	$R_L = 1\text{ M}\Omega, C_L = 60\text{ pF},$ $V_{out} = 0.3\text{ V to } (V_{CC+}) - 0.3\text{ V}$		2.5		V/ms
e_n	Equivalent input noise voltage	$f = 100\text{ Hz}$		220		nV/ $\sqrt{\text{Hz}}$
j_{e_n}	Low-frequency, peak-to-peak input noise	Bandwidth: $f = 0.1\text{ to } 10\text{ Hz}$		3.7		μV_{pp}
t_{rec}	Overload recovery time	100 mV from rail in comparator, $R_L = 100\text{ k}\Omega,$ $V_{ID} = \pm 1\text{ V}, -40\text{ }^\circ\text{C} < T < 85\text{ }^\circ\text{C}$		630		μs

1. Typical value is based on the V_{io} drift observed after 1000h at 85 °C extrapolated to 25 °C using the Arrhenius law and assuming an activation energy of 0.7 eV. The operational amplifier is aged in follower mode configuration
2. Guaranteed by design

Table 5. Electrical characteristics at (V_{CC+}) = 5 V with (V_{CC-}) = 0 V, $V_{icm} = V_{CC}/2$, $T_{amb} = 25\text{ }^\circ\text{C}$, and $R_L = 1\text{ M}\Omega$ connected to $V_{CC}/2$ (unless otherwise specified)

Symbol	Parameter	Conditions	Min.	Typ.	Max.	Unit
DC performance						
V_{io}	Input offset voltage	$T = 25\text{ }^\circ\text{C}$			150	μV
		$-40\text{ }^\circ\text{C} < T < 85\text{ }^\circ\text{C}$			235	
$\Delta V_{io}/\Delta T$	Input offset voltage drift	$-40\text{ }^\circ\text{C} < T < 85\text{ }^\circ\text{C}$			1.4	$\mu\text{V}/^\circ\text{C}$
ΔV_{io}	Long-term input offset voltage drift	$T = 25\text{ }^\circ\text{C}$ ⁽¹⁾		TBD		$\mu\text{V}/\sqrt{\text{month}}$
I_{io}	Input offset current ⁽²⁾	$T = 25\text{ }^\circ\text{C}$		1	10	pA
		$-40\text{ }^\circ\text{C} < T < 85\text{ }^\circ\text{C}$			50	
I_{ib}	Input bias current ⁽²⁾	$T = 25\text{ }^\circ\text{C}$		1	10	pA
		$-40\text{ }^\circ\text{C} < T < 85\text{ }^\circ\text{C}$			50	
CMR	Common mode rejection ratio, $20\text{ log } (\Delta V_{icm}/\Delta V_{io}),$ $V_{icm} = 0\text{ to } 3.9\text{ V}$	$T = 25\text{ }^\circ\text{C}$	90	121		dB
		$-40\text{ }^\circ\text{C} < T < 85\text{ }^\circ\text{C}$	90			
	Common mode rejection ratio, $20\text{ log } (\Delta V_{icm}/\Delta V_{io}),$ $V_{icm} = 0\text{ to } 5\text{ V}$	$T = 25\text{ }^\circ\text{C}$	85	112		
		$-40\text{ }^\circ\text{C} < T < 85\text{ }^\circ\text{C}$	80			
SVR	Supply voltage rejection ratio, $V_{CC} = 1.5\text{ to } 5.5\text{ V},$ $V_{icm} = 0\text{ V}$	$T = 25\text{ }^\circ\text{C}$	92	116		
		$-40\text{ }^\circ\text{C} < T < 85\text{ }^\circ\text{C}$	84			
A_{vd}	Large signal voltage gain, $V_{out} = 0.2\text{ V to } (V_{CC+}) - 0.2\text{ V}$	$R_L = 100\text{ k}\Omega, T = 25\text{ }^\circ\text{C}$	105	135		
		$R_L = 100\text{ k}\Omega, -40\text{ }^\circ\text{C} < T < 85\text{ }^\circ\text{C}$	101			
V_{OH}	High-level output voltage, (drop from V_{CC+})	$R_L = 10\text{ k}\Omega, T = 25\text{ }^\circ\text{C}$		10	25	mV
		$R_L = 10\text{ k}\Omega, -40\text{ }^\circ\text{C} < T < 85\text{ }^\circ\text{C}$			40	
V_{OL}	Low-level output voltage	$R_L = 10\text{ k}\Omega, T = 25\text{ }^\circ\text{C}$		7	25	
		$R_L = 10\text{ k}\Omega, -40\text{ }^\circ\text{C} < T < 85\text{ }^\circ\text{C}$			40	

Symbol	Parameter	Conditions	Min.	Typ.	Max.	Unit	
I _{out}	Output sink current, V _{out} = V _{CC} , V _{ID} = -200 mV	T = 25 °C	30	45		mA	
		-40 °C < T < 85 °C	15				
	Output source current, V _{out} = 0 V, V _{ID} = 200 mV	T = 25 °C	25	41			
		-40 °C < T < 85 °C	18				
I _{CC}	Supply current (per channel), no load, V _{out} = V _{CC} /2	T = 25 °C		950	1350	nA	
		-40 °C < T < 85 °C			1620		
AC performance							
GBP	Gain bandwidth product	R _L = 1 MΩ, C _L = 60 pF		11.5		kHz	
F _u	Unity gain frequency			10			
Φ _m	Phase margin			60			degrees
G _m	Gain margin			7			dB
SR	Slew rate (10 % to 90 %)	R _L = 1 MΩ, C _L = 60 pF, V _{out} = 0.3 V to (V _{CC+}) - 0.3 V		2.7		V/ms	
e _n	Equivalent input noise voltage	f = 100 Hz		200		nV/√Hz	
f _{e_n}	Low-frequency, peak-to-peak input noise	Bandwidth: f = 0.1 to 10 Hz		3.6		μV _{pp}	
t _{rec}	Overload recovery time	100 mV from rail in comparator, R _L = 100 kΩ, V _{ID} = ±1 V, -40 °C < T < 85 °C		940		μs	
EMIRR	Electromagnetic interference rejection ratio ⁽³⁾	V _{in} = -10 dBm, f = 400 MHz		54		dB	
		V _{in} = -10 dBm, f = 900 MHz		79			
		V _{in} = -10 dBm, f = 1.8 GHz		65			
		V _{in} = -10 dBm, f = 2.4 GHz		65			

1. Typical value is based on the V_{io} drift observed after 1000h at 85 °C extrapolated to 25 °C using the Arrhenius law and assuming an activation energy of 0.7 eV. The operational amplifier is aged in follower mode configuration
2. Guaranteed by design
3. Based on evaluations performed only in conductive mode on the TSU111ICT.

4 Electrical characteristic curves

Figure 3. Supply current vs. supply voltage

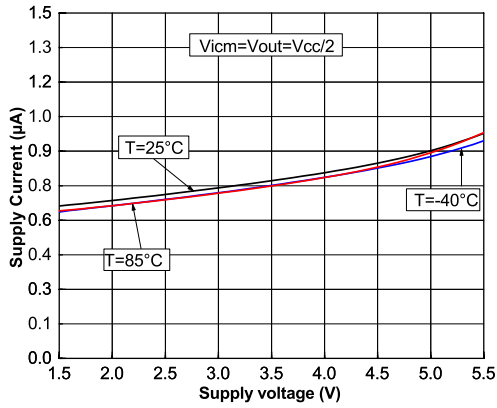


Figure 4. Supply current vs. input common-mode voltage

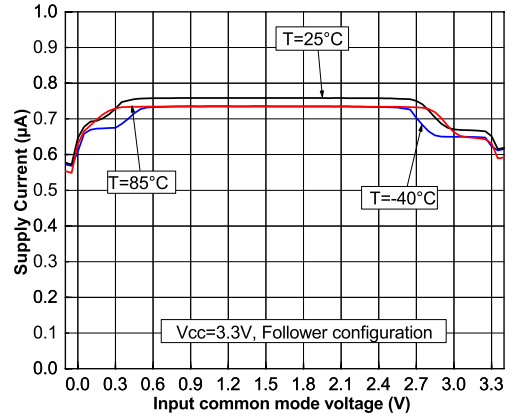


Figure 5. Input offset voltage distribution

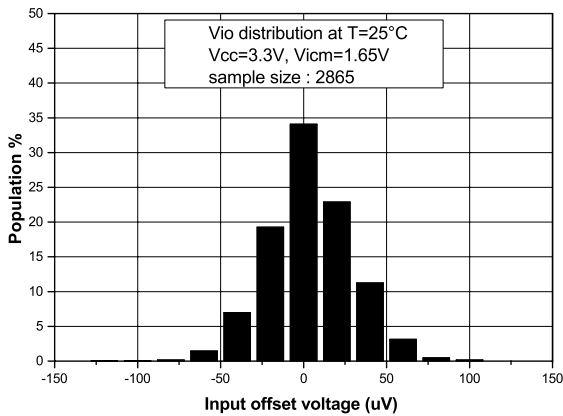


Figure 6. Input offset voltage vs. temperature at 3.3 V supply voltage

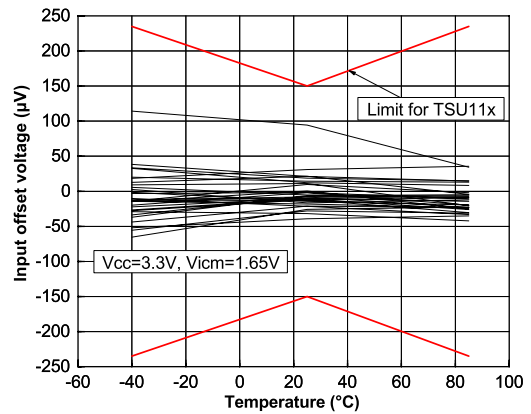


Figure 7. Input offset voltage temperature coefficient distribution from -40 °C to 25 °C

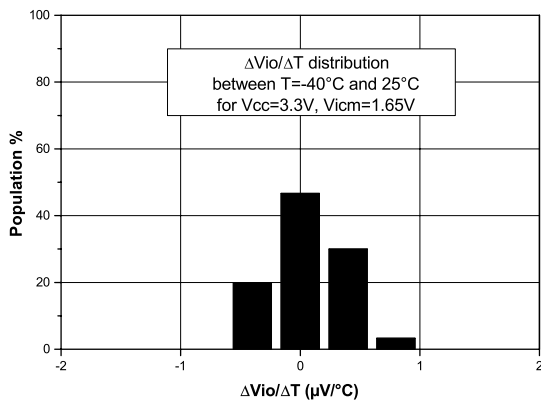


Figure 8. Input offset voltage temperature coefficient distribution from 25 °C to 85 °C

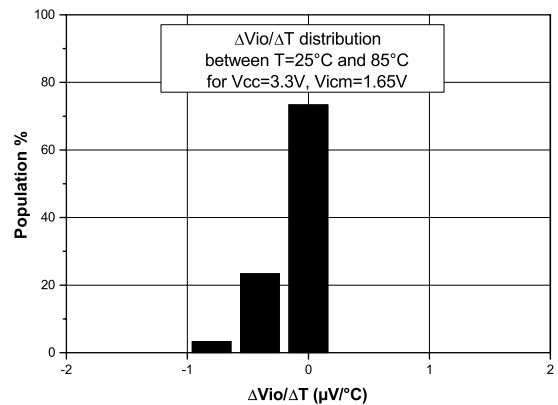


Figure 9. Input bias current vs. temperature at mid V_{ICM}

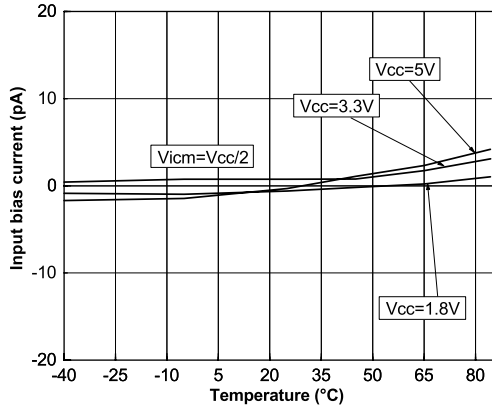


Figure 10. Input bias current vs. temperature at low V_{ICM}

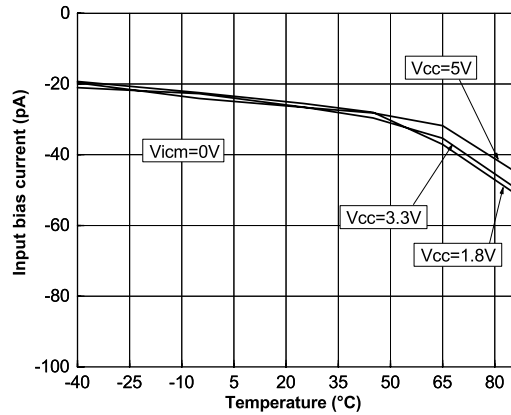


Figure 11. Input bias current vs. temperature at high V_{ICM}

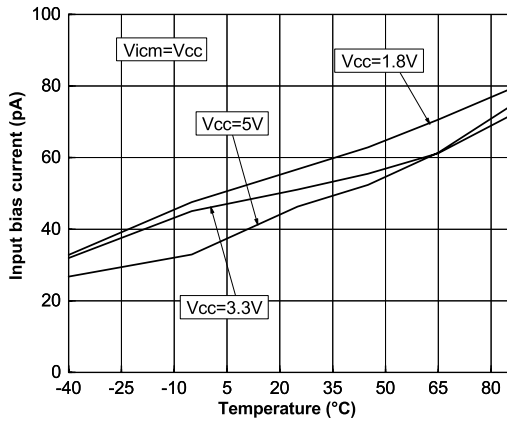


Figure 12. Output characteristics at 1.8 V supply voltage

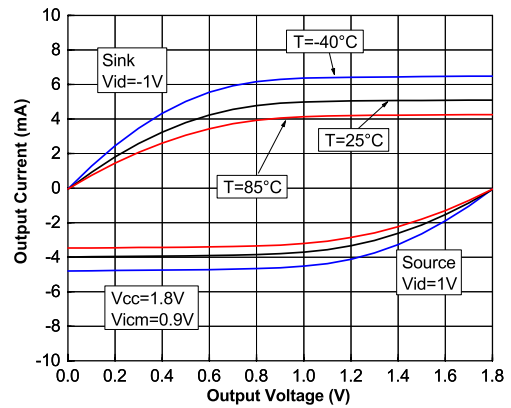


Figure 13. Output characteristics at 3.3 V supply voltage

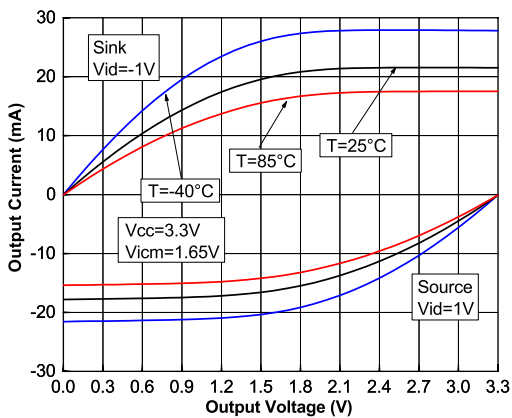


Figure 14. Output characteristics at 5 V supply voltage

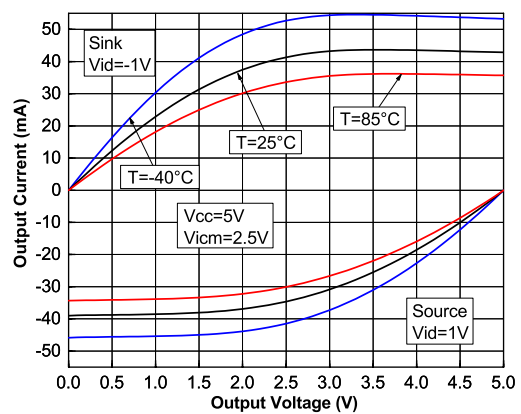


Figure 15. Output saturation with a sinewave on the input

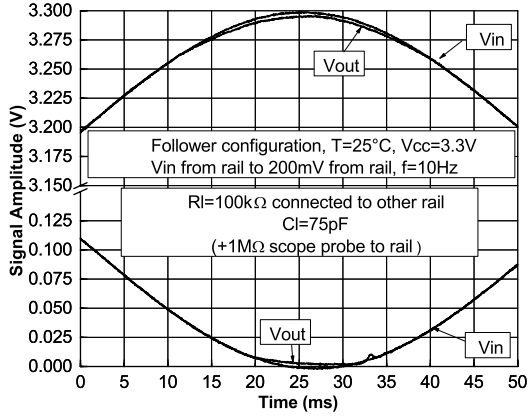


Figure 16. Output saturation with a square wave on the input

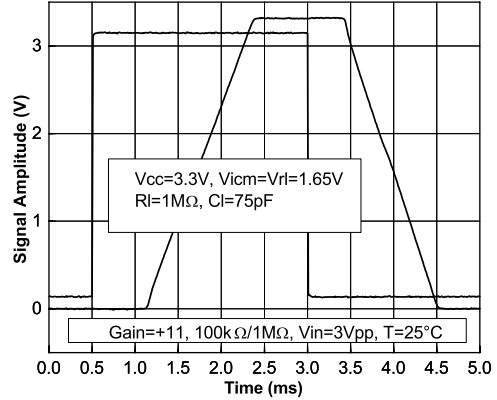


Figure 17. Phase reversal free

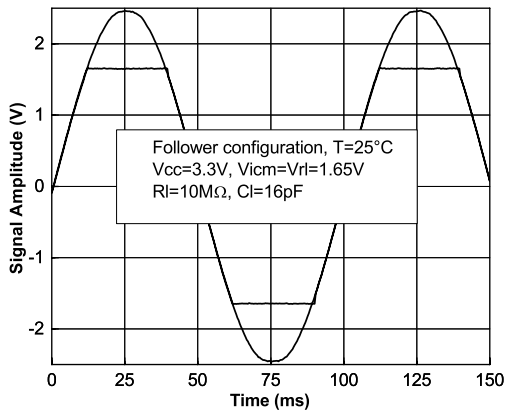


Figure 18. Slew rate vs. supply voltage

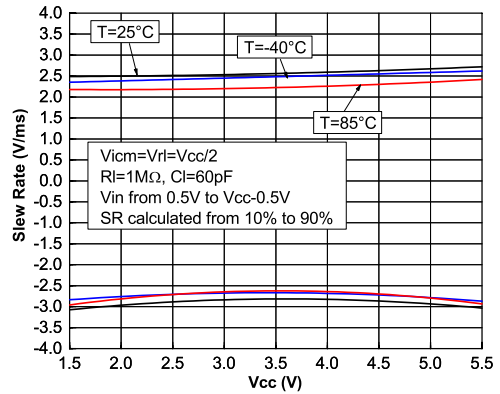


Figure 19. Output swing vs. input signal frequency

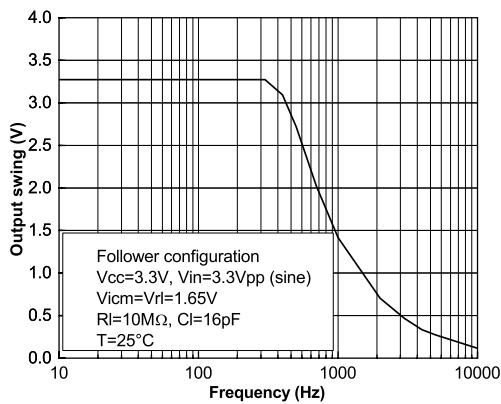


Figure 20. Triangulation of a sine wave

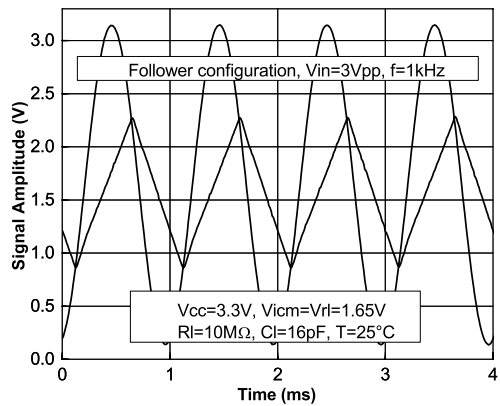


Figure 21. Large signal response at 3.3 V supply voltage

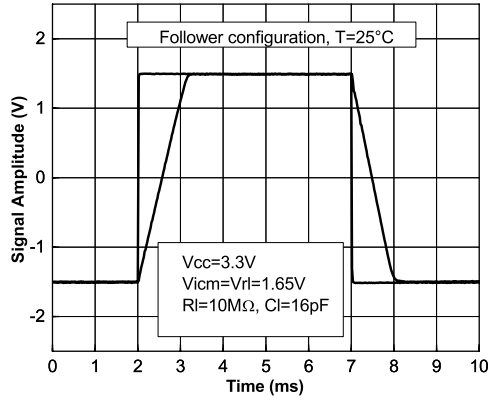


Figure 22. Small signal response at 3.3 V supply voltage

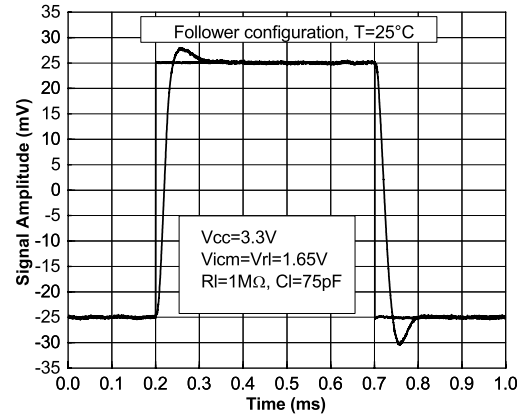


Figure 23. Overshoot vs. capacitive load at 3.3 V supply voltage

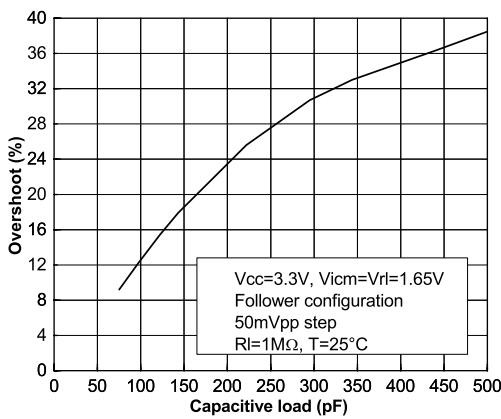


Figure 24. Open loop output impedance vs. frequency

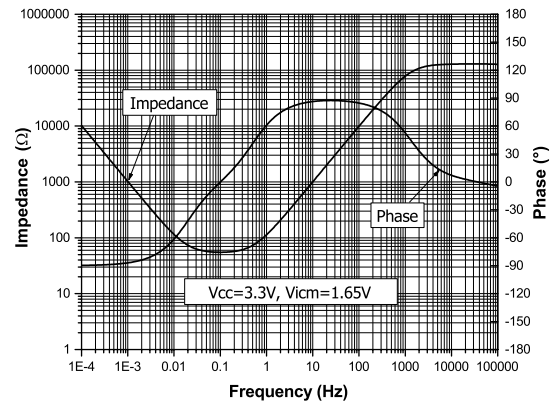


Figure 25. Bode diagram at 1.8 V supply voltage

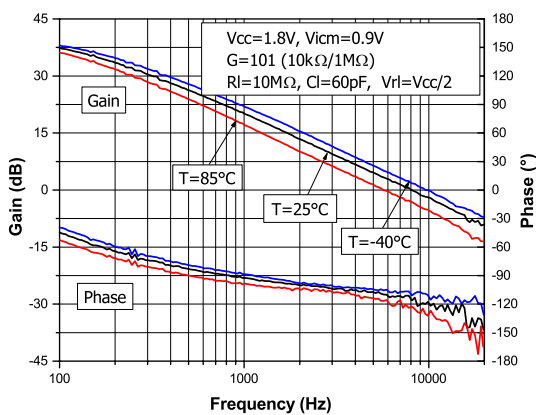


Figure 26. Bode diagram at 3.3 V supply voltage

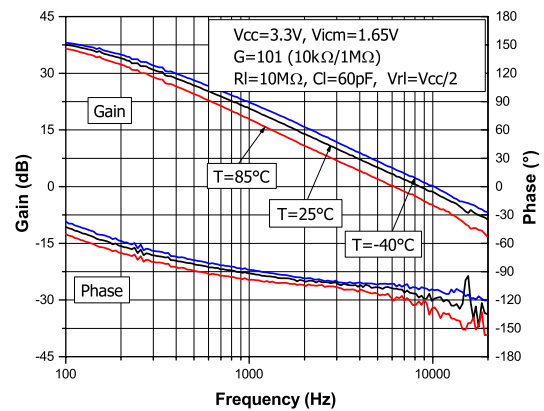


Figure 27. Bode diagram at 5 V supply voltage

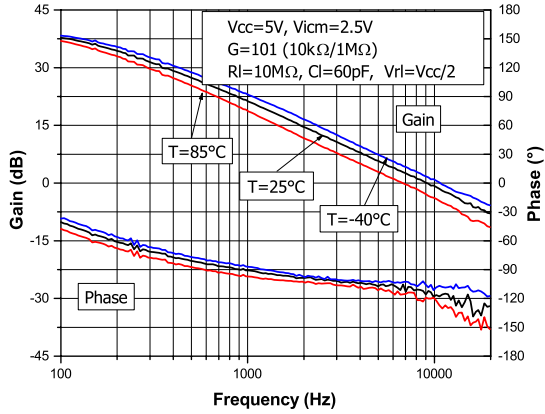


Figure 28. Gain bandwidth product vs. input common-mode voltage

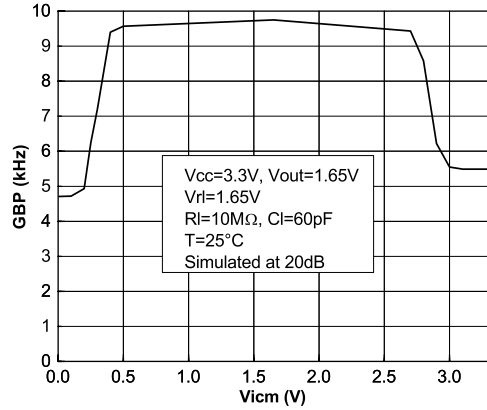


Figure 29. In-series resistor (Riso) vs. capacitive load

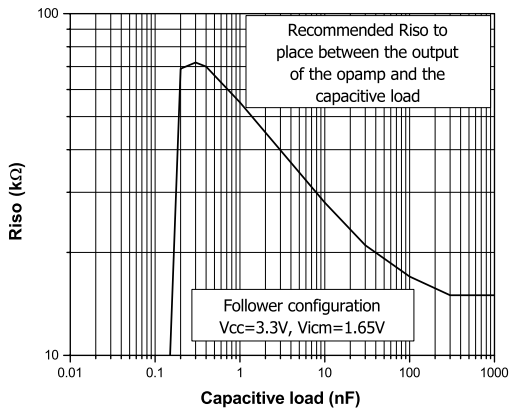


Figure 30. Noise vs. frequency for different power supply voltages

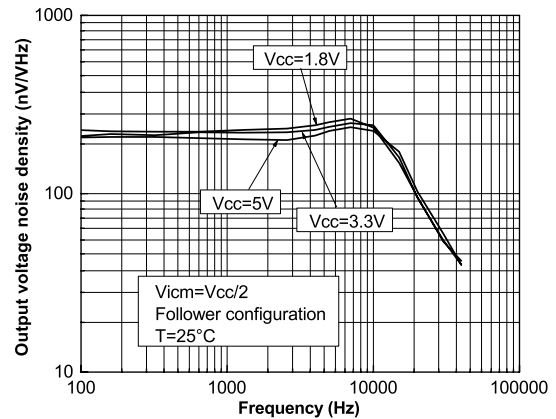


Figure 31. Noise vs. frequency for different common-mode input voltages

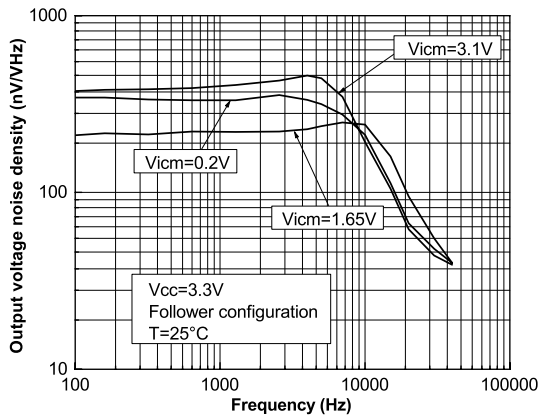
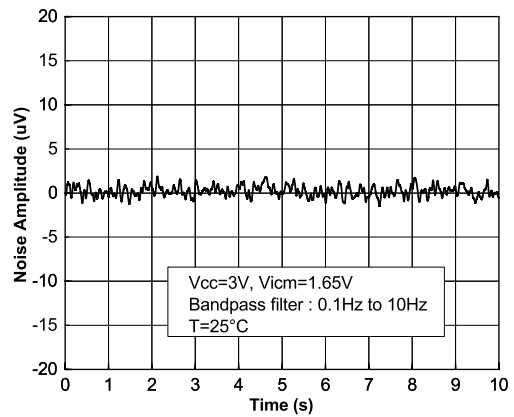


Figure 32. Noise amplitude on a 0.1 Hz to 10 Hz frequency range



5 Application information

5.1 Nanopower applications

The TSU11x can operate from 1.5 V to 5.5 V. The parameters are fully specified at 1.8 V, 3.3 V, and 5 V supply voltages and are very stable in the full V_{CC} range. Additionally, the main specifications are guaranteed on the industrial temperature range from -40 to 85 °C. The estimated lifetime of the TSU11x exceeds 25 years if supplied by a CR2032 battery (see Figure 33. CR2032 battery).

Figure 33. CR2032 battery



5.1.1 Schematic optimization aiming at nanopower

To benefit from the full performance of the TSU11x, the impedances must be maximized so that current consumption is not lost where it is not required.

For example, an aluminum electrolytic capacitance can have significantly high leakage. This leakage may be greater than the current consumption of the op-amp. For this reason, ceramic type capacitors are preferred.

For the same reason, big resistor values should be used in the feedback loop. However, there are two main limitations to be considered when choosing a resistor.

1. Noise generated: a 100 k Ω resistor generates 40 nV/ $\sqrt{\text{Hz}}$, a bigger resistor value generates even more noise.
2. Leakage on the PCB: leakage can be generated by moisture. This can be improved by using a specific coating process on the PCB.

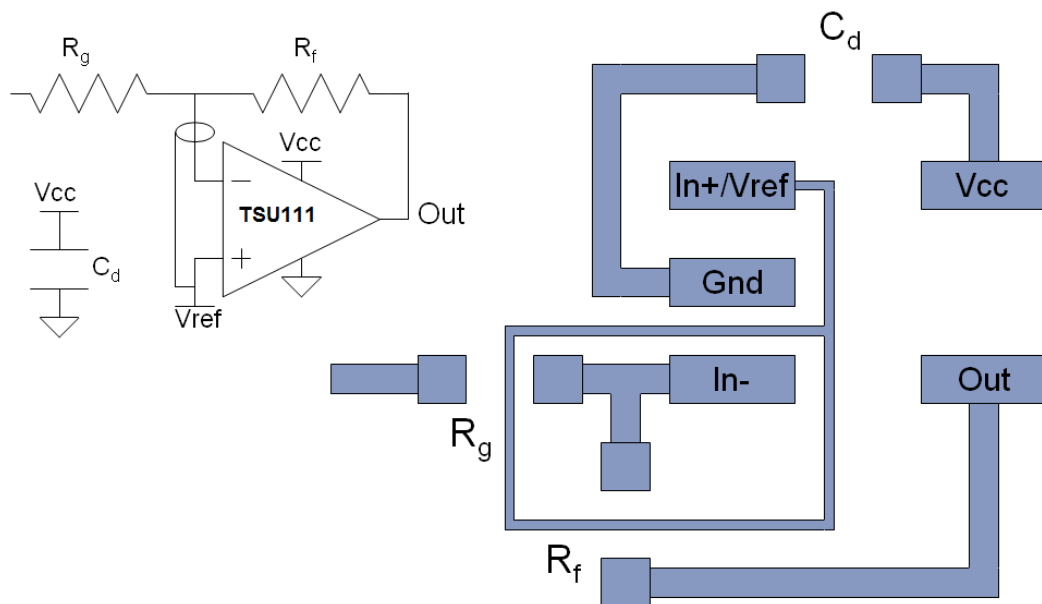
5.1.2 PCB layout considerations

For correct operation, it is advised to add 10 nF decoupling capacitors as close as possible to the power supply pins.

Minimizing the leakage from sensitive high impedance nodes on the inputs of the TSU11x can be performed with a guarding technique. The technique consists of surrounding high impedance tracks by a low impedance track (the ring). The ring is at the same electrical potential as the high impedance node.

Therefore, even if some parasitic impedance exists between the tracks, no leakage current can flow through them as they are at the same potential (see [Figure 34. Guarding on the PCB](#)).

Figure 34. Guarding on the PCB



5.2 Rail-to-rail input

The TSU11x is built with two complementary PMOS and NMOS input differential pairs. Thus, the device has a rail-to-rail input, and the input common mode range is extended from $(V_{CC-}) - 0.1 \text{ V}$ to $(V_{CC+}) + 0.1 \text{ V}$.

The TSU11x has been designed to prevent phase reversal behavior.

5.3 Input offset voltage drift overtemperature

The maximum input voltage drift variation overtemperature is defined as the offset variation related to the offset value measured at 25 °C. The operational amplifier is one of the main circuits of the signal conditioning chain, and the amplifier input offset is a major contributor to the chain accuracy. The signal chain accuracy at 25 °C can be compensated during production at application level. The maximum input voltage drift over temperature enables the system designer to anticipate the effect of temperature variations.

The maximum input voltage drift over temperature is computed using .

Equation 1

$$\frac{\Delta V_{io}}{\Delta T} = \max \left| \frac{V_{io}(T) - V_{io}(25^\circ\text{C})}{T - 25^\circ\text{C}} \right|$$

Where $T = -40^\circ\text{C}$ and 85°C .

The TSU11x datasheet maximum values are guaranteed by measurements on a representative sample size ensuring a C_{pk} (process capability index) greater than 1.3.

5.4 Long term input offset voltage drift

To evaluate product reliability, two types of stress acceleration are used:

- Voltage acceleration, by changing the applied voltage
- Temperature acceleration, by changing the die temperature (below the maximum junction temperature allowed by the technology) with the ambient temperature.

The voltage acceleration has been defined based on JEDEC results, and is defined using .

Equation 2

$$A_{FV} = e^{\beta \cdot (V_S - V_U)}$$

Where:

A_{FV} is the voltage acceleration factor

β is the voltage acceleration constant in 1/V, constant technology parameter ($\beta = 1$)

V_S is the stress voltage used for the accelerated test

V_U is the voltage used for the application

The temperature acceleration is driven by the Arrhenius model, and is defined in .

Equation 3

$$A_{FT} = e^{\frac{E_a}{k} \cdot \left(\frac{1}{T_U} - \frac{1}{T_S} \right)}$$

Where:

A_{FT} is the temperature acceleration factor

E_a is the activation energy of the technology based on the failure rate

k is the Boltzmann constant ($8.6173 \times 10^{-5} \text{ eV.K}^{-1}$)

T_U is the temperature of the die when V_U is used ($^{\circ}\text{K}$)

T_S is the temperature of the die under temperature stress ($^{\circ}\text{K}$)

The final acceleration factor, A_F , is the multiplication of the voltage acceleration factor and the temperature acceleration factor ().

Equation 4

$$A_F = A_{FT} \times A_{FV}$$

A_F is calculated using the temperature and voltage defined in the mission profile of the product. The A_F value can then be used in to calculate the number of months of use equivalent to 1000 hours of reliable stress duration.

Equation 5

$$\text{Months} = A_F \times 1000 \text{ h} \times 12 \text{ months} / (24 \text{ h} \times 365.25 \text{ days})$$

To evaluate the op amp reliability, a follower stress condition is used where V_{CC} is defined as a function of the maximum operating voltage and the absolute maximum rating (as recommended by JEDEC rules).

The V_{io} drift (in μV) of the product after 1000 h of stress is tracked with parameters at different measurement conditions (see).

Equation 6

$$V_{CC} = \max V_{op} \text{ with } V_{icm} = V_{CC} / 2$$

The long term drift parameter (ΔV_{io}), estimating the reliability performance of the product, is obtained using the ratio of the V_{io} (input offset voltage value) drift over the square root of the calculated number of months ().

Equation 7

$$\Delta V_{io} = \frac{V_{io} \text{ drift}}{\sqrt{(\text{months})}}$$

Where V_{i0} drift is the measured drift value in the specified test conditions after 1000 h stress duration.

5.5 Using the TSU11x with sensors

The TSU11x has MOS inputs, thus input bias currents can be guaranteed down to 10 pA maximum at ambient temperature. This is an important parameter when the operational amplifier is used in combination with high impedance sensors.

The TSU11x is perfectly suited for trans-impedance configuration. This configuration allows a current to be converted into a voltage value with a gain set by the user. It is an ideal choice for portable electrochemical gas sensing or photo/UV sensing applications. The TSU11x, using trans-impedance configuration, is able to provide a voltage value based on the physical parameter sensed by the sensor.

5.5.1 Electrochemical gas sensors

The output current of electrochemical gas sensors is generally in the range of tens of nA to hundreds of μ A. As the input bias current of the TSU11x is very low (see [Figure 9. Input bias current vs. temperature at mid \$V_{ICM}\$](#) , [Figure 10. Input bias current vs. temperature at low \$V_{ICM}\$](#) , and [Figure 11. Input bias current vs. temperature at high \$V_{ICM}\$](#)) compared to these current values, the TSU11x is well adapted for use with the electrochemical sensors of two or three electrodes. [Figure 36. Potentiostat schematic using the TSU111](#) shows a potentiostat (electronic hardware required to control a three electrode cell) schematic using the TSU11x. In such a configuration, the devices minimize leakage in the reference electrode compared to the current being measured on the working electrode.

Another great advantage of TSU11x versus the competition is its low noise for low frequencies (3.6 μ Vpp over 0.1 to 10 Hz), and low input offset voltage of 150 μ V max. These improved parameters for the same power consumption allow a better accuracy.

Figure 35. Trans-impedance amplifier schematic

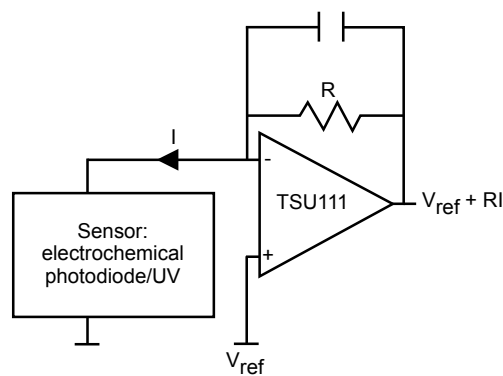
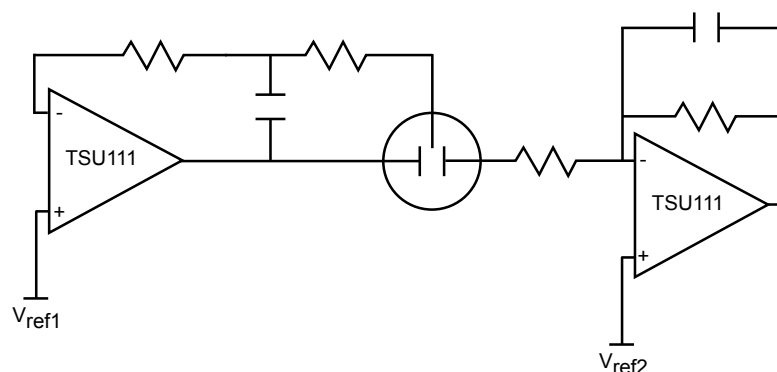


Figure 36. Potentiostat schematic using the TSU111



5.6 Fast desaturation

When the TSU11x goes into saturation mode, it takes a short period of time to recover, typically 630 μs . When recovering after saturation, the TSU11x does not exhibit any voltage peaks that could generate issues (such as false alarms) in the application (see [Figure 15. Output saturation with a sinewave on the input](#)).

We can observe that this circuit still exhibits good gain even close to the rails i.e. A_{vd} greater than 105 dB for $V_{CC} = 3.3\text{ V}$ with V_{out} varying from 200 mV up to a supply voltage minus 200 mV. With a trans-impedance schematic, a voltage reference can be used to keep the signal away from the supply rails.

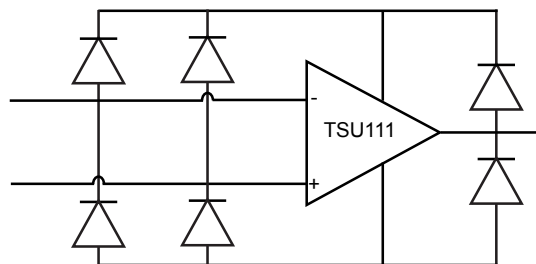
5.7 Using the TSU11x in comparator mode

The TSU11x can be used as a comparator. In this case, the output stage of the device always operates in saturation mode. In addition, [Figure 4. Supply current vs. input common-mode voltage](#) shows that the current consumption is not higher and even decreases smoothly close to the rails. The TSU11x is obviously an operational amplifier and is therefore optimized for use in linear mode. We recommend using the TS88 series of nanopower comparators if the primary function is to perform a signal comparison only.

5.8 ESD structure of the TSU11x

The TSU11x is protected against electrostatic discharge (ESD) with dedicated diodes (see [Figure 37. ESD structure](#)). These diodes must be considered at application level especially when signals applied on the input pins go beyond the power supply rails (V_{CC+}) or (V_{CC-}).

Figure 37. ESD structure



Current through the diodes must be limited to a maximum of 10 mA as stated in [Table 1. Absolute maximum ratings \(AMR\)](#). A serial resistor on the inputs can be used to limit this current.

5.9 EMI robustness of nanopower devices

Nanopower devices exhibit higher impedance nodes and consequently they are more sensitive to EMI. To improve the natural robustness of the TSU11x device, we recommend to add three capacitors of around 22 pF each between the two inputs, and between each input and ground. These capacitors lower the impedance of the input at high frequencies and therefore reduce the impact of the radiation.

6 Package information

In order to meet environmental requirements, ST offers these devices in different grades of ECOPACK® packages, depending on their level of environmental compliance. ECOPACK® specifications, grade definitions and product status are available at: www.st.com. ECOPACK® is an ST trademark.

6.1 SC70-5 (or SOT323-5) package information (TSU111)

Figure 38. SC70-5 (or SOT323-5) package outline

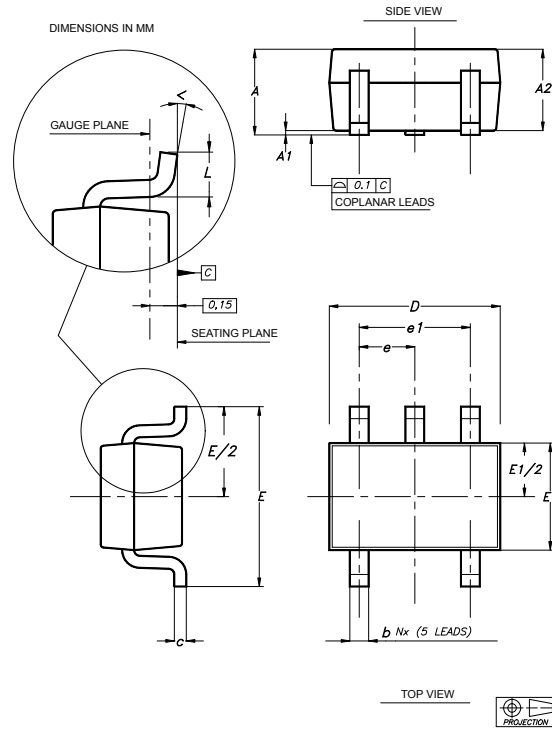


Table 6. SC70-5 (or SOT323-5) package mechanical data

Ref.	Dimensions					
	Millimeters			Inches		
	Min.	Typ.	Max.	Min.	Typ.	Max.
A	0.80		1.10	0.032		0.043
A1			0.10			0.004
A2	0.80	0.90	1.00	0.032	0.035	0.039
b	0.15		0.30	0.006		0.012
c	0.10		0.22	0.004		0.009
D	1.80	2.00	2.20	0.071	0.079	0.087
E	1.80	2.10	2.40	0.071	0.083	0.094
E1	1.15	1.25	1.35	0.045	0.049	0.053
e		0.65			0.025	
e1		1.30			0.051	
L	0.26	0.36	0.46	0.010	0.014	0.018
<	0°		8°	0°		8°

6.2 DFN6 1.2x1.3 package information (TSU111)

Figure 39. DFN6 1.2x1.3 package outline

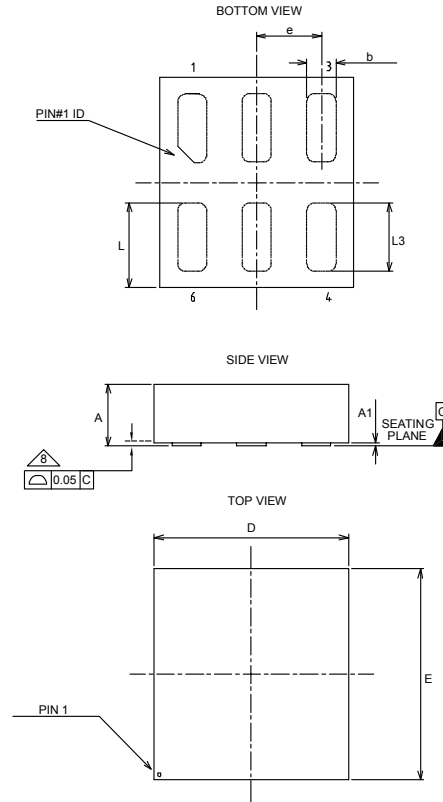


Table 7. DFN6 1.2x1.3 mechanical data

Ref	Dimensions					
	Millimeters			Inches		
	Min.	Typ.	Max.	Min.	Typ.	Max.
A	0.31	0.38	0.40	0.012	0.015	0.016
A1	0.00	0.02	0.05	0.000	0.001	0.002
b	0.15	0.18	0.25	0.006	0.007	0.010
c		0.05			0.002	
D		1.20			0.047	
E		1.30			0.051	
e		0.40			0.016	
L	0.475	0.525	0.575	0.019	0.021	0.023
L3	0.375	0.425	0.475	0.015	0.017	0.019

Figure 40. DFN6 1.2x1.3 recommended footprint

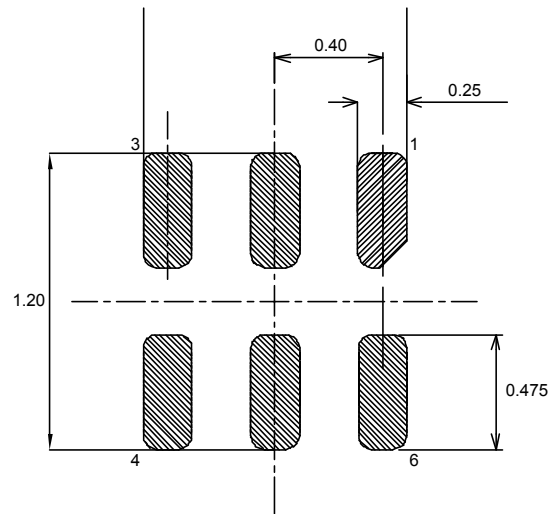


Table 8. DFN6 1.2x1.3 recommended footprint data

Ref.	Dimensions	
	Millimeters	Inches
A	4.00	0.158
B		
C	0.50	0.020
D	0.30	0.012
E	1.00	0.039
F	0.70	0.028
G	0.66	0.026

6.3 MiniSO8 package information (TSU112)

Figure 41. MiniSO8 package outline

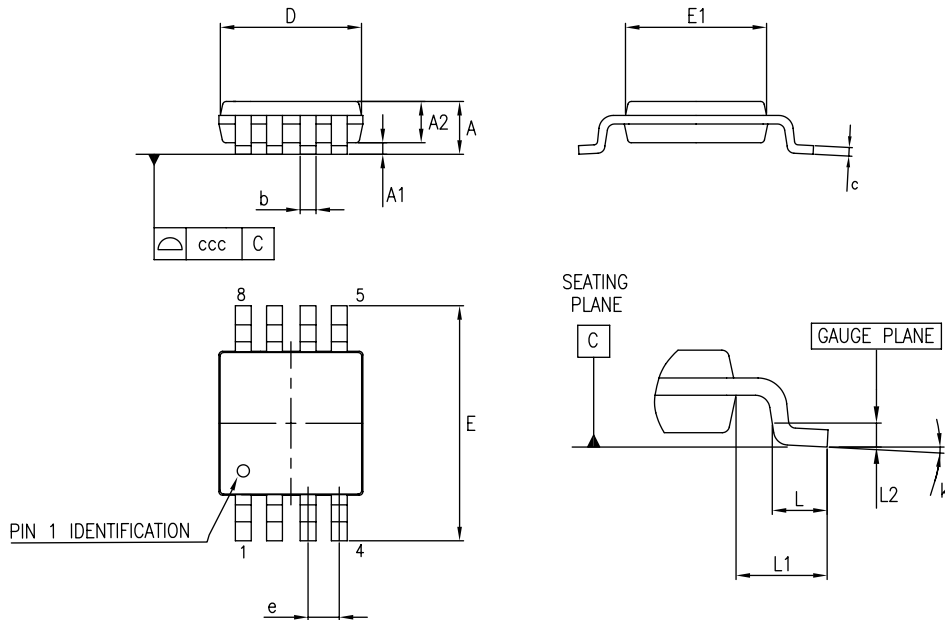


Table 9. MiniSO8 mechanical data

Dim.	Millimeters			Inches		
	Min.	Typ.	Max.	Min.	Typ.	Max.
A			1.1			0.043
A1	0		0.15	0		0.006
A2	0.75	0.85	0.95	0.03	0.033	0.037
b	0.22		0.4	0.009		0.016
c	0.08		0.23	0.003		0.009
D	2.8	3	3.2	0.11	0.118	0.126
E	4.65	4.9	5.15	0.183	0.193	0.203
E1	2.8	3	3.1	0.11	0.118	0.122
e		0.65			0.026	
L	0.4	0.6	0.8	0.016	0.024	0.031
L1		0.95			0.037	
L2		0.25			0.01	
k	0°		8°	0°		8°
ccc			0.1			0.004

6.4 DFN8 2x2 package information (TSU112)

Figure 42. DFN8 2x2 package outline

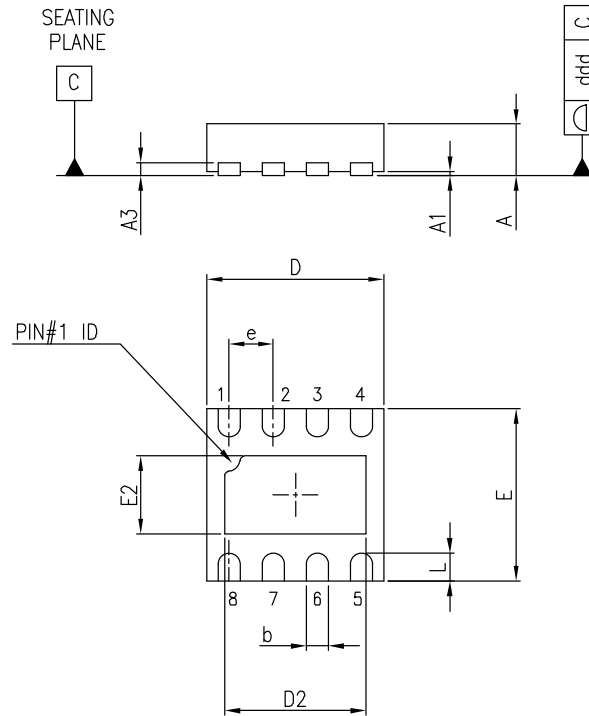
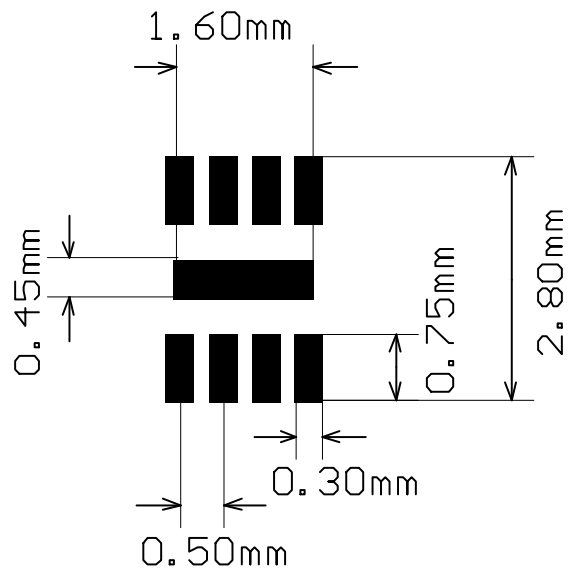


Table 10. DFN8 2x2 package mechanical data

Ref.	Dimensions					
	Millimeters			Inches		
	Min.	Typ.	Max.	Min.	Typ.	Max.
A	0.51	0.55	0.60	0.020	0.022	0.024
A1			0.05			0.002
A3		0.15			0.006	
b	0.18	0.25	0.30	0.007	0.010	0.012
D	1.85	2.00	2.15	0.073	0.079	0.085
D2	1.45	1.60	1.70	0.057	0.063	0.067
E	1.85	2.00	2.15	0.073	0.079	0.085
E2	0.75	0.90	1.00	0.030	0.035	0.039
e		0.50			0.020	
L	0.225	0.325	0.425	0.009	0.013	0.017
ddd			0.08			0.003

Figure 43. DFN8 2x2 recommended footprint



7 Ordering information

Table 11. Order code

Order code	Temperature range	Package ⁽¹⁾	Marking
TSU111IQ1T	-40 °C to 85 °C	DFN6 1.2x1.3	K8
TSU111ICT		SC70-5	
TSU112IQ2T		DFN8 2x2	K37
TSU112IST		MiniSO8	

1. All devices are delivered in tape and reel packing.

Revision history

Table 12. Document revision history

Date	Revision	Changes
17-Oct-2016	1	Initial release
14-Nov-2016	2	Features: added "rail-to-rail input and output". Description: updated the maximum ultra low-power consumption of TSU111 op-amp. Applications: updated Table 5: added EMIRR typ. values Added Section 5.9: "EMI robustness of nanopower devices".
04-Dec-2017	3	Added the part number TSU112 and the relative package information MiniSO8 and DFN8 2x2.
08-May-2018	4	Updated Section 3 Electrical characteristics .

Contents

1	Package pin connections	2
2	Absolute maximum ratings and operating conditions	3
3	Electrical characteristics	4
4	Electrical characteristic curves	8
5	Application information	13
5.1	Nanopower applications	13
5.1.1	Schematic optimization aiming at nanopower	13
5.1.2	PCB layout considerations	14
5.2	Rail-to-rail input	14
5.3	Input offset voltage drift overtemperature	14
5.4	Long term input offset voltage drift	15
5.5	Using the TSU11x with sensors	16
5.5.1	Electrochemical gas sensors	16
5.6	Fast desaturation	16
5.7	Using the TSU11x in comparator mode	17
5.8	ESD structure of the TSU11x	17
5.9	EMI robustness of nanopower devices	17
6	Package information	18
6.1	SC70-5 (or SOT323-5) package information (TSU111)	19
6.2	DFN6 1.2x1.3 package information (TSU111)	19
6.3	MiniSO8 package information (TSU112)	21
6.4	DFN8 2x2 package information (TSU112)	22
7	Ordering information	25
	Revision history	26

List of tables

Table 1.	Absolute maximum ratings (AMR)	3
Table 2.	Operating conditions	3
Table 3.	Electrical characteristics at (V_{CC+}) = 1.8 V with (V_{CC-}) = 0 V, $V_{icm} = V_{CC}/2$, $T_{amb} = 25\text{ }^{\circ}\text{C}$, and $R_L = 1\text{ M}\Omega$ connected to $V_{CC}/2$ (unless otherwise specified)	4
Table 4.	Electrical characteristics at (V_{CC+}) = 3.3 V with (V_{CC-}) = 0 V, $V_{icm} = V_{CC}/2$, $T_{amb} = 25\text{ }^{\circ}\text{C}$, and $R_L = 1\text{ M}\Omega$ connected to $V_{CC}/2$ (unless otherwise specified)	5
Table 5.	Electrical characteristics at (V_{CC+}) = 5 V with (V_{CC-}) = 0 V, $V_{icm} = V_{CC}/2$, $T_{amb} = 25\text{ }^{\circ}\text{C}$, and $R_L = 1\text{ M}\Omega$ connected to $V_{CC}/2$ (unless otherwise specified)	6
Table 6.	SC70-5 (or SOT323-5) package mechanical data	19
Table 7.	DFN6 1.2x1.3 mechanical data	20
Table 8.	DFN6 1.2x1.3 recommended footprint data	21
Table 9.	MiniSO8 mechanical data	22
Table 10.	DFN8 2x2 package mechanical data	23
Table 11.	Order code	25
Table 12.	Document revision history	26

List of figures

Figure 2.	Pin connections for each package (top view)	2
Figure 3.	Supply current vs. supply voltage	8
Figure 4.	Supply current vs. input common-mode voltage	8
Figure 5.	Input offset voltage distribution	8
Figure 6.	Input offset voltage vs. temperature at 3.3 V supply voltage	8
Figure 7.	Input offset voltage temperature coefficient distribution from -40 °C to 25 °C	8
Figure 8.	Input offset voltage temperature coefficient distribution from 25 °C to 85 °C	8
Figure 9.	Input bias current vs. temperature at mid V_{ICM}	9
Figure 10.	Input bias current vs. temperature at low V_{ICM}	9
Figure 11.	Input bias current vs. temperature at high V_{ICM}	9
Figure 12.	Output characteristics at 1.8 V supply voltage	9
Figure 13.	Output characteristics at 3.3 V supply voltage	9
Figure 14.	Output characteristics at 5 V supply voltage	9
Figure 15.	Output saturation with a sinewave on the input	10
Figure 16.	Output saturation with a square wave on the input	10
Figure 17.	Phase reversal free	10
Figure 18.	Slew rate vs. supply voltage	10
Figure 19.	Output swing vs. input signal frequency	10
Figure 20.	Triangulation of a sine wave	10
Figure 21.	Large signal response at 3.3 V supply voltage	11
Figure 22.	Small signal response at 3.3 V supply voltage	11
Figure 23.	Overshoot vs. capacitive load at 3.3 V supply voltage	11
Figure 24.	Open loop output impedance vs. frequency	11
Figure 25.	Bode diagram at 1.8 V supply voltage	11
Figure 26.	Bode diagram at 3.3 V supply voltage	11
Figure 27.	Bode diagram at 5 V supply voltage	12
Figure 28.	Gain bandwidth product vs. input common-mode voltage	12
Figure 29.	In-series resistor (Riso) vs. capacitive load	12
Figure 30.	Noise vs. frequency for different power supply voltages	12
Figure 31.	Noise vs. frequency for different common-mode input voltages	12
Figure 32.	Noise amplitude on a 0.1 Hz to 10 Hz frequency range	12
Figure 33.	CR2032 battery	13
Figure 34.	Guarding on the PCB	14
Figure 35.	Trans-impedance amplifier schematic	16
Figure 36.	Potentiostat schematic using the TSU111	16
Figure 37.	ESD structure	17
Figure 38.	SC70-5 (or SOT323-5) package outline	19
Figure 39.	DFN6 1.2x1.3 package outline	20
Figure 40.	DFN6 1.2x1.3 recommended footprint	21
Figure 41.	MiniSO8 package outline	22
Figure 42.	DFN8 2x2 package outline	23
Figure 43.	DFN8 2x2 recommended footprint	24

IMPORTANT NOTICE – PLEASE READ CAREFULLY

STMicroelectronics NV and its subsidiaries (“ST”) reserve the right to make changes, corrections, enhancements, modifications, and improvements to ST products and/or to this document at any time without notice. Purchasers should obtain the latest relevant information on ST products before placing orders. ST products are sold pursuant to ST’s terms and conditions of sale in place at the time of order acknowledgement.

Purchasers are solely responsible for the choice, selection, and use of ST products and ST assumes no liability for application assistance or the design of Purchasers’ products.

No license, express or implied, to any intellectual property right is granted by ST herein.

Resale of ST products with provisions different from the information set forth herein shall void any warranty granted by ST for such product.

ST and the ST logo are trademarks of ST. All other product or service names are the property of their respective owners.

Information in this document supersedes and replaces information previously supplied in any prior versions of this document.

© 2018 STMicroelectronics – All rights reserved